3D Multisource Full-Waveform Inversion using Dynamic Random Phase Encoding

Chaiwoot Boonyasiriwat and Gerard T. Schuster, King Abdullah University of Science and Technology*

Summary

We have developed a multisource full-waveform inversion algorithm using a dynamic phase encoding strategy with dual-randomization—both the position and polarity of simultaneous sources are randomized and changed every iteration. The dynamic dual-randomization is used to promote the destructive interference of crosstalk noise resulting from blending a large number of common shot gathers into a supergather. We compare our multisource algorithm with various algorithms in a numerical experiment using the 3D SEG/EAGE overthrust model and show that our algorithm provides a higher-quality velocity tomogram than the other methods that use only mono-randomization. This suggests that increasing the degree of randomness in phase encoding should improve the quality of the inversion result.

Introduction

Full-waveform inversion (FWI) is a method for inverting seismic data for a model of subsurface structures, e.g., velocity models, used for seismic imaging. For synthetic data, a velocity model estimated from FWI has a resolution high enough for seismic interpretation as demonstrated by the synthetic data results in Bunks et al. (1995), Sirgue and Pratt (2004), Brenders and Pratt (2007), and Boonyasiriwat et al. (2009b). However, FWI is still computationally expensive and many efforts have aimed to improve its computational efficiency, including multisource methods (Vigh and Starr, 2008; Ben-Hadj-Ali et al., 2009a,b; Krebs et al., 2009; Zhan et al., 2009).

In the work of Vigh and Starr (2008), linear time shifts or slant stacking are used to encode a large number of common shot gathers into a smaller number of supergathers resulting to a significant reduction in the number of forward modeling required or a large computational gain. This strategy is commonly known as plane-wave source phase encoding, and is suitable for marine applications. However, when applied to land data with complex near-surface subsurface structures and rugged topography, plane-wave phase encoding is not practical.

Instead of using a deterministic phase encoding strategy as in plane-wave FWI of Vigh and Starr (2008), we can use stochastic or random phase encoding strategies (Romero et al., 2000; Ben-Hadj-Ali et al., 2009a,b; Krebs et al., 2009; Zhan et al., 2009). Random phase encoding can be applied to both marine and land data applications, and is simple and straightforward to implement for FWI. In the work of Zhan et al. (2009), random time shifts are used for phase encoding with a special preconditioner to help multisource FWI to converge. Krebs et al. (2009) solve the convergence problem by changing encryption codes every iteration. In their work, a random amplitude encoding was used, and it was found that randomizing the polarity of each simultaneous source was an efficient multisource strategy. This means all sources have the same signature except the polarity which is randomly assigned. In addition, a degree of randomness is added in their method by changing the encryption code every iteration so that crosstalk noise is reduced by destructive interference. However, all of the shot gathers are stacked together to form just one supergather for their multisource FWI. Although this could yield a large speedup factor, we suspect that multisource FWI using only one supergather may not always provide an accurate inversion result or may have a convergence problem. This leads to our work that compares the method of Krebs et al. (2009) to multisource FWI methods using multiple supergathers with additional randomization.

In this paper, we improve the efficiency of 3D multisource FWI using a dual-randomization strategy. Our method is a combination of the dynamic amplitude encoding strategy of Krebs et al. (2009) and the randomization of source and receiver positions used in 3D Kirchhoff migration by Sun et al. (1997) and Zhou et al. (1999). In addition, our methods use multiple supergathers instead of using only one supergather, and each supergather is generated by a selected set of sources, not all sources.

We propose to maximize the phase differences between traces in different shot gathers as much as possible. Such difference will enhance the reduction of crosstalk noise in the FWI image. This can be accomplished by randomizing the phase of each shot and the location of each shot every iteration. In this work, the Halton quasi-random number generator (Niederreiter, 1992) is used to select the locations of simultaneous sources. Other random number generators can be used also but the Halton method used in the work of Sun et al. (1997) provided cleaner migration images compared to those using a regular distribution of sources and receivers.

This paper is divided into six parts. The first part is the summary followed by the introduction. In the next part, the theory of multisource FWI using the acoustic approximation is described. Then we show numerical results from a synthetic experiment using the 3D SEG/EAGE overthrust model followed by the conclusion and acknowledgment sections.

Multisource Full-Waveform Inversion

In this section, we present the theory of multisource acoustic FWI. We begin by recalling the conventional FWI method. In FWI, the velocity model is updated by minimizing the misfit function, defined here as the L_2-norm of the data residuals:

$$E = \frac{1}{2}\sum_{s=1}^{N_s}\sum_{g=1}^{N_g}\int \left[p_{obs}(\mathbf{r}_g,t|\mathbf{r}_s) - p_{calc}(\mathbf{r}_g,t|\mathbf{r}_s)\right]^2 dt, \quad (1)$$

where $p_{obs}(\mathbf{r}_g,t|\mathbf{r}_s)$ and $p_{calc}(\mathbf{r}_g,t|\mathbf{r}_s)$ are the observed and calculated data, respectively, recorded at time t by a geophone at $\mathbf{r}_g$ from a source excitation at $\mathbf{r}_s$.

The gradient of the misfit function is computed by the zero-lag correlation between the forward-propagated wavefields and back-projected wavefield residuals (Tarantola, 1984; Luo and Schuster, 1991; Zhou et al., 1995, 1997; Sheng et al., 2006; Boonyasiriwat et al., 2009a):

$$g(\mathbf{r}) = \frac{2}{c(\mathbf{r})} \sum_{s=1}^{N_s} \int \dot{p}(\mathbf{r},t|\mathbf{r}_s) \dot{p}'(\mathbf{r},t|\mathbf{r}_s) dt, \tag{2}$$

where $\dot{p}$ denotes the time derivative of p, $p(\mathbf{r},t|\mathbf{r}_s)$ represents the forward-propagated wavefields given by

$$p(\mathbf{r},t|\mathbf{r}_s) = \int G(\mathbf{r},t|\mathbf{r}',0) * S(\mathbf{r}',t|\mathbf{r}_s) d\mathbf{r}', \tag{3}$$

and $p'(\mathbf{r},t|\mathbf{r}_s)$ represents the back-projected wavefield residuals given by

$$p'(\mathbf{r},t|\mathbf{r}_s) = \int G(\mathbf{r},-t|\mathbf{r}',0) * \delta S(\mathbf{r}',t|\mathbf{r}_s) d\mathbf{r}'. \tag{4}$$

Here, $G(\mathbf{r},t|\mathbf{r}',0)$ is the Green's function, the symbol $*$ represents temporal convolution, $S(\mathbf{r},t|\mathbf{r}_s)$ and $\delta S(\mathbf{r},t|\mathbf{r}_s)$ are the source functions of the forward-propagated wavefields and back-projected wavefield residuals, respectively, and

$$\delta S(\mathbf{r}',t|\mathbf{r}_s) = \sum_{g=1}^{N_g} \delta(\mathbf{r}'-\mathbf{r}_g)[p_{obs}(\mathbf{r}_g,t|\mathbf{r}_s) - p_{calc}(\mathbf{r}_g,t|\mathbf{r}_s)]. \tag{5}$$

It is well known that the computational cost per iteration of computing the gradient in equation 2 is roughly about three times that of forward modeling. In 3D applications, the cost of gradient computation is prohibitive and causes FWI to be impractical. Significant cost reduction can be obtained by simultaneously using multiple sources in the gradient computation, instead of using separate sources. This is accomplished by phase encoding both forward-propagated wavefields and back-projected wavefield residuals:

$$\tilde{p}(\mathbf{r},t|s') = \sum_{s=1}^{N_s} a(s'|\mathbf{r}_s) p(\mathbf{r},t|\mathbf{r}_s) \tag{6}$$

and

$$\tilde{p'}(\mathbf{r},t|s') = \sum_{s=1}^{N_s} a(s'|\mathbf{r}_s) p'(\mathbf{r},t|\mathbf{r}_s), \tag{7}$$

where $a(s'|\mathbf{r}_s)$ is a phase-encoding function. Minimizing the difference between observed and calculated phase-encoded supergathers leads to multisource FWI whose misfit function and gradient can be written, respectively, as

$$\tilde{E} = \frac{1}{2} \sum_{s'=1}^{N_{s'}} \sum_{g=1}^{N_g} \int \left[\tilde{p}_{obs}(\mathbf{r}_g,t|s') - \tilde{p}_{calc}(\mathbf{r}_g,t|s')\right]^2 dt \tag{8}$$

and

$$\tilde{g}(\mathbf{r}) = \frac{2}{c(\mathbf{r})} \sum_{s'=1}^{N_{s'}} \int \dot{\tilde{p}}(\mathbf{r},t|s') \dot{\tilde{p}}'(\mathbf{r},t|s') dt, \tag{9}$$

where $N_{s'}$ is the number of supergathers which is normally much smaller than N_s. Therefore, the cost of gradient computation in multisource FWI is reduced by a factor of $\approx N_s/N_{s'}$ due to the fact that the cost of phase encoding is negligible compared to that of gradient computation (Krebs et al., 2009).

In our multisource FWI algorithm, the random phase-encoding function incorporates both polarity and location of simultaneous sources, and has the form,

$$a(s'|\mathbf{r}_s) = \begin{cases} 0 & ; s \in I(s') \\ (-1)^i & ; s \in A(s'), i \in Z^+ \end{cases} \tag{10}$$

Here $I(s')$ is the set of inactive source indices, $A(s')$ is the set of active source indices which is randomly generated by the Halton quasi-random number generator, and i is a random number and a positive integer (Z^+). Sets $I(s')$ and $A(s')$ have the following properties:

$$I(s') \cup A(s') = \{1,2,...,N_s\}, \tag{11}$$

and

$$A(s'_1) \cap A(s'_2) = \begin{cases} A(s'_1) & ; s'_1 = s'_2 \\ \emptyset & ; s'_1 \neq s'_2 \end{cases} \tag{12}$$

Equation 12 also implies that

$$\bigcup_{s'=1}^{N_{s'}} A(s') = \{1,2,...,N_s\}. \tag{13}$$

The encoding function $a(s'|\mathbf{r}_s)$ randomly changes the polarity of the active sources. In practice, shots are not located on a Halton set of points, so a nearest-neighbor interpolation method is used to select the shot location on a regular grid that is nearest to the Halton point.

Numerical Results: 3D SEG/EAGE Overthrust Model

An acoustic synthetic data set is generated from the 3D SEG/EAGE overthrust model (Figure 1a) whose grid size is $800 \times 800 \times 186$ and spatial sampling interval is 20 m. The 5-Hz Ricker wavelet is used as the source time function, and a fixed-spread acquisition geometry is used in this experiment as previously used in the work of Krebs et al. (2009). There are 1089 sources (N_s = 1089) evenly distributed along the surface with an interval of 500 m in the inline (X) and crossline (Y) directions. Conventional FWI using separate sources is not used in this work due to its computational cost. Multisource FWI using the Krebs method, static and dynamic QMC encoding with and without random source polarity (RSP) are applied to this data set to test our conjecture that the dynamic QMC phase encoding with RSP (dynamic dual-random phase encoding) will converge faster and provide a higher-quality inversion result than the other methods. In the QMC phase encoding methods, 11 supergathers ($N_{s'}^{QMC}$ = 11) are used with 99 simultaneous sources in a supergather while all 1089 sources are used simultaneously in the Krebs method ($N_{s'}^{Krebs}$ = 1).

Compared to conventional single-source FWI, multisource FWI has some overhead due to the encoding of common shot gathers into supergathers during each iteration. However, this overhead is negligible compared to the cost of computing the gradient; therefore, multisource FWI has a speedup per iteration

equal to the number of simultaneous sources (Krebs et al., 2009). Since conventional FWI is not used here, the speedup factors of the QMC methods and the Krebs method are theoretically estimated as equal to 99 and 1089, respectively.

The initial velocity model used is the smoothed version of the true velocity. The inversion is carried out for 40 iterations for all methods using 4096 processors on an IBM Blue Gene/P system, and provides the velocity tomograms shown in Figure 1. The tomogram from the dynamic QMC method with RSP (Figure 1d) has the best image quality compared to tomograms obtained from the other methods (inversion results using QMC encoding without RSP are not shown here). This is obvious when comparing the depth slices. In addition, using multiple supergathers provide inversion results with less artifacts than using only one supergather.

All methods have a comparable convergence rate in the data space. The dynamic QMC and Krebs methods have jumpy data-fit curves due to the fact that the data are re-encoded every iteration where the residual is computed with respect to the encoded data at the current iteration. At the next iteration, the same model can result in a different data residual with respect to the new encoded data. This phonomenon can also be seen in the work of Krebs et al. (2009).

Conclusions

We have compared multisource full-waveform inversion (FWI) methods with different phase encoding strategies. Multisource FWI using only one supergather is the most computationally efficient but may result to an inversion result with strong artifacts. By using more supergathers, multisource FWI provides higher-quality velocity tomograms with an extra cost, i.e., about three times slower than using one supergather in our experiment. In the dynamic QMC phase encoding with random source polarity, dual randomization is used in the inversion and provides a higher-quality inversion result and a slightly higher convergence rate than using mono-randomization. This suggests a multifolding strategy where the initial iterations might use one supergather that is a stack of all shot gathers, while the later iterations use fewer shot gathers in forming multiple supergathers.

Acknowledgements

We are grateful for the support from the members of the University of Utah Tomography and Modeling/Migration Consortium. We would like to thank Aron Ahmadia and Mark Cheeseman for their helpful support and expertise on high-performance computation, Iain Georgeson and Jonathan Anderson for their administrative support on Shaheen, Ge Zhan and Wei Dai for useful discussions on multisource methods, and Benoit Marchand for Linux workstation supports.

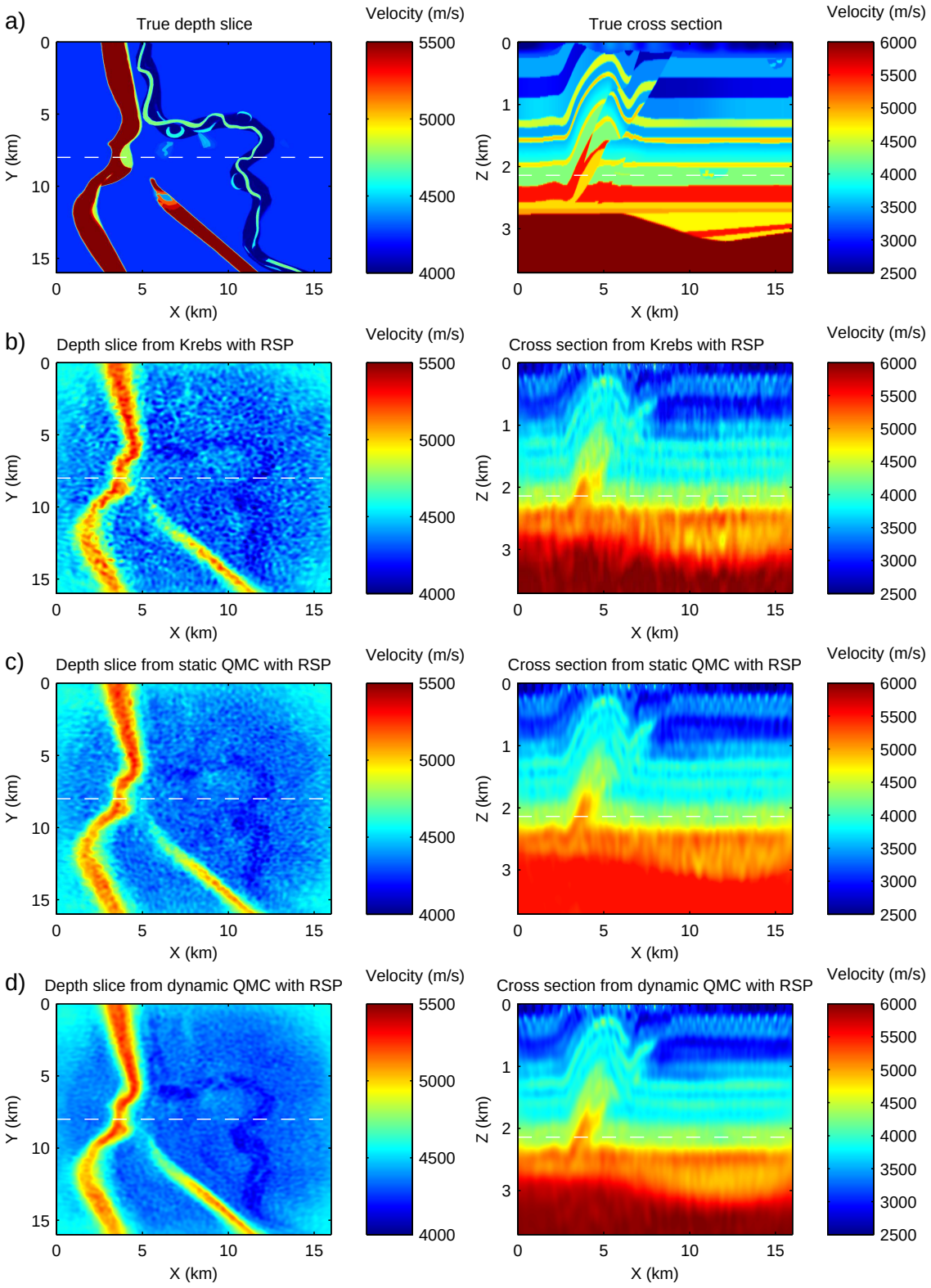

Figure 1: Depth slices at $z = 2.1$ km and cross-sections at $y = 8$ km of a) true model, and inverted models using random source polarity (RSP) in b) the Krebs method, c) static QMC method, and d) dynamic QMC method.

EDITED REFERENCES

Note: This reference list is a copy-edited version of the reference list submitted by the author. Reference lists for the 2010 SEG Technical Program Expanded Abstracts have been copy edited so that references provided with the online metadata for each paper will achieve a high degree of linking to cited sources that appear on the Web.

REFERENCES

Ben-Hadj-Ali, H., S. Operto, and J. Virieux, 2009a, Efficient 3D frequency-domain full waveform inversion (FWI) with phase encoding: Presented at the 71st Annual International Meeting, EAGE.

--------, 2009b, Three-dimensional frequency-domain full waveform inversion with phase encoding: SEG Expanded Abstracts, **28**, 2288.

Boonyasiriwat, C., P. Valasek, P. Routh, W. Cao, G. T. Schuster, and B. Macy, 2009a, An efficient multiscale method for time-domain waveform tomography: Geophysics, **74**, no. 6, WCC59–WCC68, doi:10.1190/1.3151869.

Boonyasiriwat, C., P. Valasek, P. Routh, and X. Zhu, 2009b, Application of multiscale waveform tomography for high-resolution velocity estimation in complex geologic environments: Canadian foothills synthetic data example: The Leading Edge, **28**, no. 4, 454–456, doi:10.1190/1.3112764.

Brenders, A. J., and R. G. Pratt, 2007, Full waveform tomography for lithospheric imaging: Results from a blind test in a realistic crustal model: Geophysical Journal International, **168**, no. 1, 133–151, doi:10.1111/j.1365-246X.2006.03156.x.

Bunks, C., F. M. Saleck, S. Zaleski, and G. Chavent, 1995, Multiscale seismic waveform inversion: Geophysics, **60**, 1457–1473, doi:10.1190/1.1443880.

Krebs, J. R., J. E. Anderson, D. Hinkley, R. Neelamani, S. Lee, A. Baumstein, and M. D. Lacasse, 2009, Fast full-wavefield seismic inversion using encoded sources: Geophysics, **74**, no. 6, WCC177–WCC188, doi:10.1190/1.3230502.

Luo, Y., and G. T. Schuster, 1991, Wave equation traveltime inversion: Geophysics, **56**, 645–653, doi:10.1190/1.1443081.

Niederreiter, H., 1992, Random number generation and quasi-Monte Carlo methods: SIAM Press.

Romero, L. A., D. C. Ghiglia, C. C. Ober, and S. A. Morton, 2000, Phase encoding of shot records in prestack migration: Geophysics, **65**, 426–436, doi:10.1190/1.1444737.

Sheng, J., A. Leeds, M. Buddensiek, and G. T. Schuster, 2006, Early arrival waveform tomography on near-surface refraction data: Geophysics, **71**, no. 4, U47–U57, doi:10.1190/1.2210969.

Sirgue, L., and R. G. Pratt, 2004, Efficient waveform inversion and imaging: A strategy for selecting temporal frequencies: Geophysics, **69**, 231–248, doi:10.1190/1.1649391.

Sun, Y., G. T. Schuster, and K. Sikorski, 1997, A quasi-Monte Carlo approach to 3-D migration: Theory: Geophysics, **62**, 918–928, doi:10.1190/1.1444199.

Tarantola, A., 1984, Inversion of seismic reflection data in the acoustic approximation: Geophysics, **49**, 1259–1266, doi:10.1190/1.1441754.

Vigh, D., and E. W. Starr, 2008, 3D prestack plane-wave, full-waveform inversion: Geophysics, **73**, no. 5, VE135–VE144, doi:10.1190/1.2952623.

Zhan, G., W. Dai, and G. T. Schuster, 2009, Acoustic multisource waveform inversion with deblurring: Journal of Seismic Exploration.

Zhou, C., W. Cai, Y. Luo, G. T. Schuster, and S. Hassanzadeh, 1995, Acoustic wave-equation traveltime and waveform inversion of crosshole seismic data: Geophysics, **60**, 765–773, doi:10.1190/1.1443815.

Zhou, C., J. Chen, G. T. Schuster, and B. A. Smith, 1999, A quasi-Monte Carlo approach to efficient 3-D migration: Field data test: Geophysics, **62**, 918–928.

Zhou, C., G. T. Schuster, S. Hassanzadeh, and J. M. Harris, 1997, Elastic wave equation traveltime and waveform inversion of crosswell data: Geophysics, **62**, 853–868, doi:10.1190/1.1444194.